Iron-Chromium-Carbon System at 870°C

L. RICHARD WOODYATT AND GEORGE KRAUSS

A series of 13 Fe-Cr-C alloys was studied to determine the phases present after the alloys were equilibrated for 1000 h at 870°C (1600°F). The alloys had a nominal composition of 1 pct carbon and 0 to 29 pct chromium. The experimental program employed: a) selective etching plus X-ray diffraction studies of extracted carbides to identify the carbides, b) quantitative metallography plus electrolytic carbide extraction to determine the quantity of carbides, and c) electron microprobe analyses plus chemical analyses of extracted carbides to determine the carbide compositions. Microprobe traverses through the carbide particles and the adjoining matrices showed that equilibrium had been established. The M_3C, M_7C_3 and $M_{23}C_6$ carbides were all stoichiometric with respect to carbon—in contrast to most prior diagrams which show the M_3C and M_7C_3 forming a pseudobinary system.

THE Fe-Cr-C system has been investigated many times over the past 40 years. However, most studies have dealt with portions of the system far removed from the alloy composition ranges and annealing temperatures used in commercial stainless and tool steels. The studies of Tofaute *et al*[1-2] and Bungardt *et al*[3] were notable exceptions in that they dealt with 850°C (1560°C) isothermal sections. Likewise, Jackson[4] published a 900°C (1650°F) isothermal section. In a recent review Forgeng and Forgeng[5] found that: 1) the only carbides present were M_3C, M_7C_3 and $M_{23}C_6$, 2) the M_3C and M_7C_3 form a pseudobinary system, and 3) the $M_{23}C_6$ carbides are in equilibrium with both austenite and ferrite, whereas the M_3C and M_7C_3 carbides are in equilibrium with austenite only.

Benz *et al*[6] concluded that the 900°C (1650°F) isothermal section is similar to the 850°C section described by Forgeng. However, they considered M_3C and M_7C_3 to be stoichiometric carbides (*cf* Jackson[4]), and found that the solubility limits of iron in M_7C_3 and $M_{23}C_6$ were 57.9 and 42.7 pct respectively, *i.e.*, higher than the 37.2 and 24.5 pct proposed by Forgeng and Forgeng. Although Benz and his coworkers did use microprobe analysis extensively in their study in contrast to previous studies based on chemical and X-ray analysis of extracted carbides, they did not use microprobe analysis to determine carbon contents.

The purpose of this investigation was to determine as completely as possible the Fe-Cr-C 870°C isothermal section, a temperature of interest for tool steel and stainless steel heat treatment. The composition limits of 0 to 30 pct Cr bracket the levels of those elements that are found in both groups of steels, and 1 pct C is typical of tool steels and wear-resistant stainless steels. Microprobe analysis for Fe, Cr and C as well as a variety of other experimental techniques were used to obtain information about the structure, quantity and compositions of the phases present in each alloy.

L. RICHARD WOODYATT is Engineer, Bethlehem Steel Corporation, Homer Research Laboratories, Bethlehem, PA 18016. GEORGE KRAUSS is AMAX Foundation Professor, Department of Metallurgical Engineering, Colorado School of Mines, Golden, CO 80401.

Manuscript submitted October 7, 1975.

EXPERIMENTAL TECHNIQUES

The specific steps in the experimental program were:

- Selective etching of metallographic specimens and X-ray diffraction studies of extracted carbides to identify the types of carbides present in the alloys.
- The carbide quantities were determined by quantitative metallography and the weight percentage of extracted carbides.
- Electron microprobe analyses and chemical analyses to determine carbide compositions.
- Finally, matrix compositions were determined by microprobe analyses and the materials balance between alloy composition and the volume and composition of the carbides.

Materials and Heat Treatment

All alloys were produced as 22 Kg (50 lb) air-induction-melted heats. Their compositions are listed in Table I. The raw materials were high-carbon Sorrel Iron to provide the carbon and a portion of the iron, low-carbon 50 pct ferrochrome, and low-carbon Armco Iron for the balance of the iron. The bars were forged to a diameter of 2.54 mm (1 in.) at temperatures between 1065°C (1950°F) and 1145°C (2100°F). After homogenization for 12 to 14 h at 1140°C (2075°F), the bars were ground to 20 mm (0.75 in.), sealed in evacu-

Table I. Chemical Analyses of the Alloys

Alloy	C	Cr	Mn	Ni
C1	0 96	1 30	0 41	0.08
C2	1 03	3.05	0 15	0.10
C3	0 90	3.86	0 18	0 08
C4	1.06	3 99	0.13	0.08
C5	1.03	4.71	0 16	0.10
C6	0.97	5 06	0 15	0.06
C7	1.02	7 72	0 14	0.10
C8	1.07	13.14	0 17	0.12
C9	0.95	17 00	0.19	0.15
C10	1 18	20.11	0 19	0 15
C11	0.95	21.39	0.19	0.16
C12	0.94	23 93	0 22	0.20
C13	1 00	28 87	0.24	0 14

ated quartz tubes backfilled with 10 KPa (0.1 atm) high-purity argon, and annealed for 1000 h at 870°C. Finally, slices 5 mm (0.2 in.) thick were cut from the middle of each annealed bar, reheated to 870°C (1600°F) and oil-quenched to suppress carbide precipitation during cooling.

Carbide Extraction

The carbides were extracted from the quenched slices by anodic dissolution of the matrix in a 10 pct HCl/methyl alcohol electrolyte.[7] The weighed specimens had an active surface area of 300 mm.^{2} Stainless strips of comparable surface area were the cathodes. Electrolysis was performed at a current density of 75 to 100 mA/cm^2 for 6 h. After the electrolysis, the adhering residue was removed from the specimen with a glass rod and an ultrasonic cleaner. The extracted residue was separated from the electrolyte by centrifuging. After drying, the centrifuge tube containing the residue was weighed and the weight percentage of the residue was calculated by dividing the weight gain of the centrifuge tube by the weight loss of the specimen.

X-Ray Diffraction

The X-ray diffraction of the extraction residues was done on a General Electric XRD-6 diffractometer with chromium radiation, a vanadium filter, and operating conditions of 45 kV at 20 mA. Representative X-ray diffraction patterns are shown in Fig. 1. All diffraction patterns were indexed in accordance with data from the ASTM Powder Diffraction File.[8] All lines in the patterns were accounted for, except for the single line at a d spacing of 2.124Å (0.2124 nm) in the $M_{23}C_6$ pattern in Fig. 1(d). Although, as shown in Fig. 1(b), M_7C_3 carbides have a line with d spacing of 2.12Å, the absence of the strong lines at d spacings of 2.28, 1.96, 1.75, 1.71, 1.44 and 1.38Å indicates that the unknown line was not emitted from M_7C_3 carbides. A line with d = 2.12Å also appears in the X-ray pattern from the iron-chromium sigma phase (Reference Card 5-0708[8]). However, the absence of the strong lines at d spacings of 2.063, 1.964 and 1.928Å shows that the sigma phase is not the source of the unknown line. The lattice parameters for the carbides were calculated by adapting Hess's modification of Cohen's method[9] to a least-squares linear regression computer program.

Electron Microprobe Analysis

The compositions of the carbides and matrix phases were determined by electron microprobe analysis on ARL-EMX microprobes. A lithium fluoride (LiF) crystal spectrometer was used to analyze the CrKα and FeKα radiations, and the CKα radiation was analyzed with either a lead stearate crystal spectrometer or a blazed-grating spectrometer. All work was done at an operating potential of 10 kV and a specimen current of 0.1 μA. The counting times for all measurements were 80 to 100 s. When a crystal spectrometer was used in an analysis, background readings were taken at an off-peak position. However, for carbon analyses with the grating spectrometer, the very broad peak made it necessary to do the carbon background measurements on-peak on the pure iron standard. Finally, carbon contamination during the long counting times was determined from a curve of carbon pickup as a function of counting time and was sub-

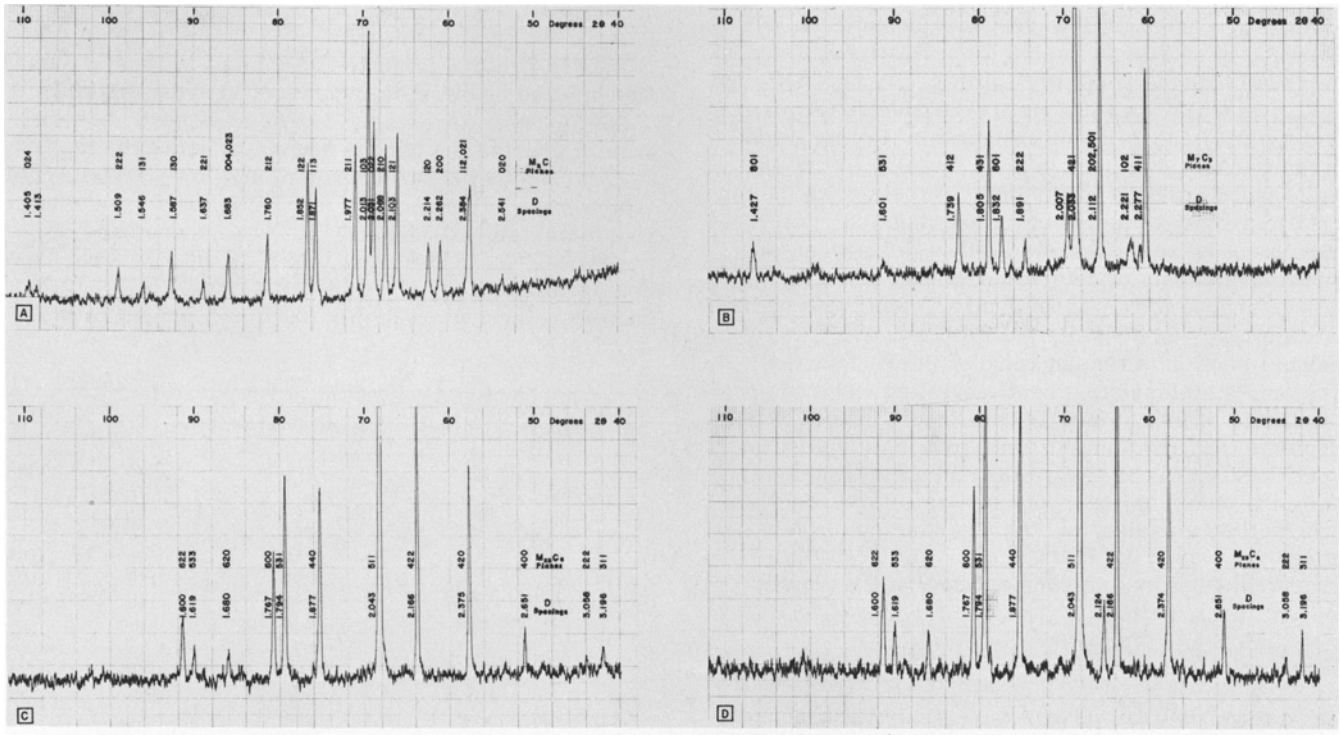

Fig. 1—Representative X-ray diffraction charts of extracted carbides; (a) M_3C in Alloy C1 (0.96 pct C, 1.30 pct Cr), (b) M_7C_3 in Alloy C6 (0.97 pct C, 5.06 pct Cr), (c) $M_{23}C_6$ in Alloy C11 (0.95 pct C, 21.39 pct Cr), (d) $M_{23}C_6$ in Alloy C13 (1.00 pct C, 28.87 pct Cr).

tracted from all carbon readings. All probe analyses were limited to carbides and carbide-free matrix areas larger than 4 μm. Quantitative analyses were made with standard procedures to correct the data for atomic number effects, X-ray absorption, and secondary fluorescence. These corrections were made with the computer program developed by Goldstein *et al*[10] after modifications to incorporate the carbon absorption coefficients reported by Henke *et al*.[11] The microprobe results were *not* normalized to total 100 pct.

The standards for all samples were Johnson-Matthey iron, Johnson-Matthey molybdenum, and spectrographically pure chromium. A sample of quenched high-purity Fe-1.00 pct C steel was the standard for matrix carbon contents, while cementite in a spheroidized sample of the same Fe-1.00 pct C steel was the standard for carbide carbon contents.

Metallography

The type and volume of each carbide and matrix phase were determined by selective etching with the etchants listed in Table II. In specimens containing both ferrite and martensite, tempering for 1 h at 200°C (400°F) was used to darken the martensite. The total volume percent of carbides in each alloy was measured with a Quantimet 720 image analyzer operating at a magnification of 360 times with a field size of 0.25 mm square and a resolution of 0.43 μm. Each of the results presented is the average of 25 readings. No selective etch was found that would distinguish the different carbides sufficiently for use of the Quantimet. Therefore, carbide volumes in selectively etched specimens were determined by manual point-counting.

RESULTS AND DISCUSSION

Before discussing the experimentally determined 870°C section of the Fe-Cr-C system, we will first summarize preliminary work performed to determine: a) whether there was a measureable segregation of the major impurity elements, *e.g.*, manganese, and nickel, to either the matrix or the carbides, and b) whether the alloys were at equilibrium after 1000 h at 870°C (1600°F).

Distribution of Mn and Ni

The alloys, as shown in Table I, contained 0.13 to 0.41 pct Mn and 0.06 to 0.20 pct Ni. Generally, the manganese was combined in sulfide inclusions. However, it was not known whether the nickel and possibly some of the manganese would segregate strongly to either the carbide or the matrix and thus affect carbide formation and/or equilibrium. Therefore, the distribution of these elements was studied in alloy C13 (1.00 pct C, 28.87 pct Cr) after equilibration for 1000 h at 870°C (1600°F). This alloy was chosen because it contained large, well-defined carbides and significant amounts of Mn and Ni.

The distribution ratios of manganese and nickel, *i.e.*, the concentration of each element in the carbide divided by its concentration in the matrix, were determined by quantitative microprobe analysis to be, respectively, 1.26 and 0.82. These ratios are consistent with: a) the observations of Gurry[12] that manganese concentrates in cementite whereas nickel concentrates in the ferrite, and b) the findings of Clayton *et al*[13] that the cementite/ferrite partitioning ratios for manganese range from 1.27 to 1.44 whereas those for nickel range from 0.77 to 0.94. However, since the concentrations of these elements were quite low, we concluded that partitioning ratios of these magnitudes would not significantly affect the equilibration or carbide formation in the alloys.

Table II. Response to Selective Etchants

Etchant	M_3C	M_7C_3	$M_{23}C_6$
Chromic acid composition = 1 g CrO_3 + 100 ml H_2O used electrolytically at 30 V etch for 30 s	Not attacked	Outlined in black	Outlined in black
Murakami's reagent composition = 10 g $K_3Fe(CN)_6$ + 10 g KOH + 100 ml H_2O etch for 10 s	Not attacked	Not attacked	Colored light tan
Potassium permanganate composition = 4 g $KMnO_4$ + 4 g NaOH + 100 ml H_2O etch for 20 s	Not attacked	Not attacked	Colored light tan

Attainment of Equilibrium

The attainment of equilibrium in the alloys held for 1000 h at 870°C (1600°F) was confirmed by making microprobe readings at 1 μm intervals across the

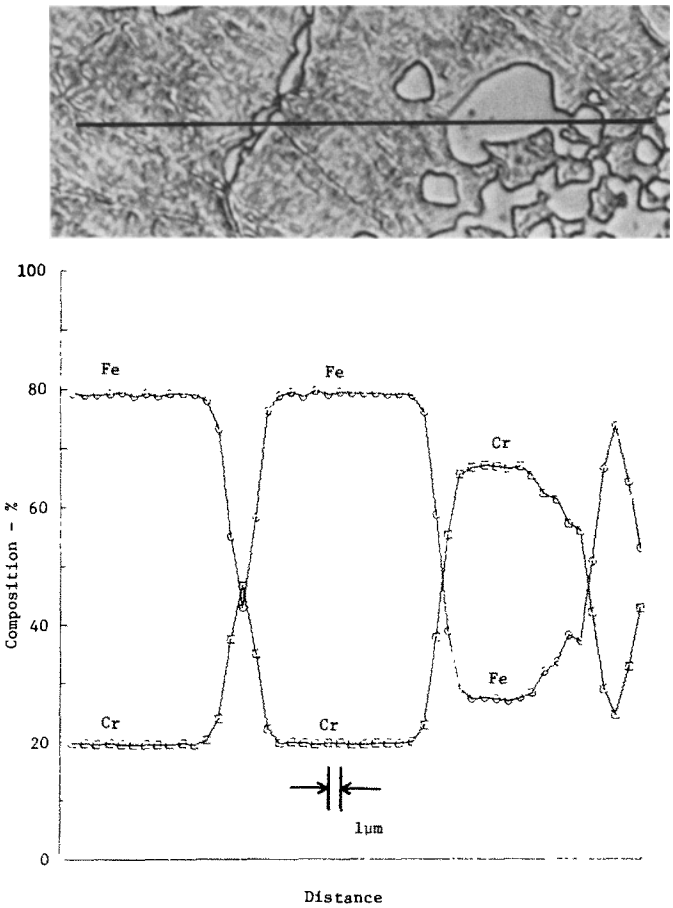

Fig. 2—Composition profile of Alloy C13 (1.00 pct C, 28.87 pct Cr) held for 250 h at 870°C (1600°F).

specimens of alloy C13. As shown in the concentration profiles of Figs. 2 and 3, no gradients were found in the matrices, evidence that equilibrium had been attained. The carbides were generally too small for determination of concentration gradients. The composition profile for a specimen held 250 h at 870°C (1600°F) is quite similar to that shown in Fig. 3 for the same alloy held 1000 h at 870°C. In both cases, the chromium contents of the matrix and carbides, 19.5 and 68.0 pct respectively, were virtually the same as the 19.74 and 68.58 reported in Table VI for the $M_{23}C_6$ carbides, obtained by microprobe analyses. Measurements had to be made at least 2 μm away from the interface between two phases to eliminate effects of the other phase.

Iron-Chromium-Carbon System

The 870°C (1600°F) isothermal section of the iron-chromium-carbon system determined in this study is shown in Fig. 4. Enlargements of the low-carbon, low-chromium region and the high-carbon region of the isothermal section are shown in Figs. 5 and 6, respectively. Included in Figs. 5 and 6 are the boundaries of the phase fields determined by other investigators. The results of X-ray diffraction studies of extracted carbides are shown in Table III, and the amounts and average compositions of the extracted carbides are listed in Tables IV and V, respectively. Finally, the microprobe analyses of carbides and matrices are listed in Table VI, and representative micrographs of the two- and three-phase alloys are shown in Fig. 7. Each of the tie lines in Fig. 4 was determined by calculating a least-squares line that went through the composition of the alloy as well as the compositions of its carbide and matrix phases. Similarly, the sides of the tie triangles were determined by calculating a least-squares line through the compositions of the component phases. Finally, the carbide phase bound-

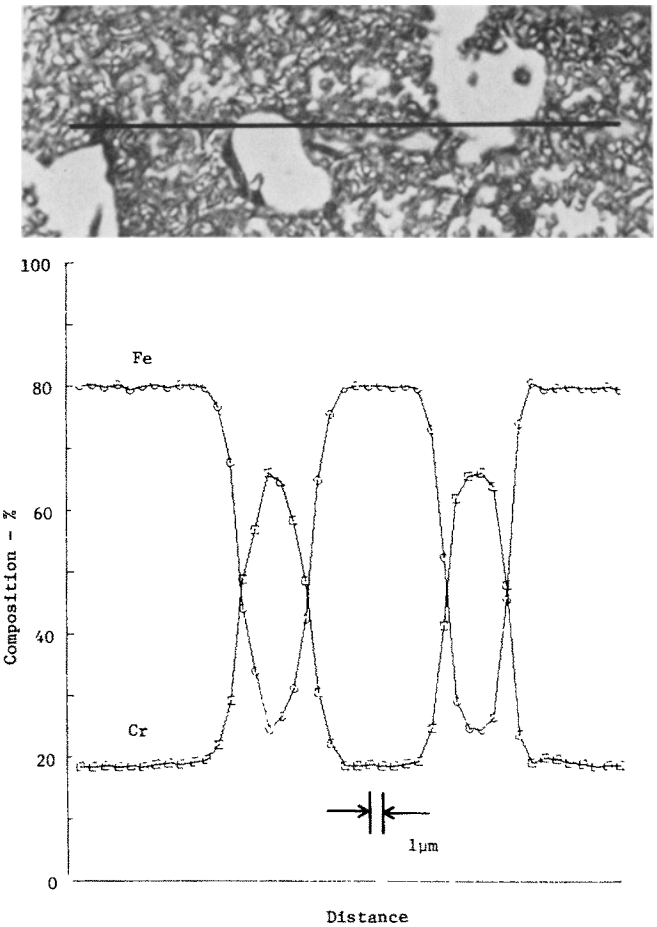

Fig. 3—Composition profile of Alloy C13 (1.00 pct C, 28.87 pct Cr) held 1000 h at 870°C (1600°F).

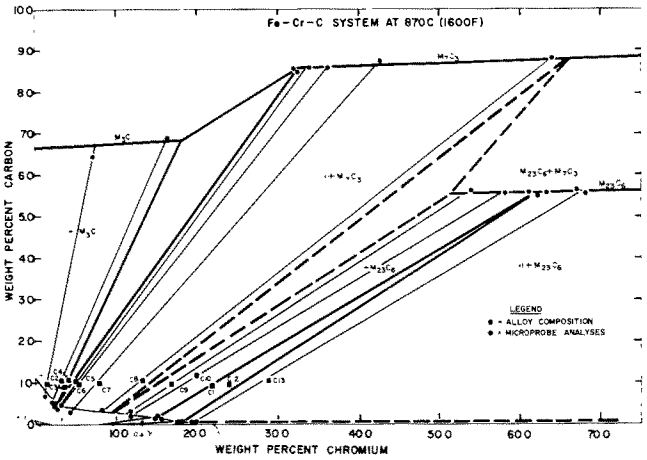

Fig. 4—The 870°C (1600°F) isothermal section of the Fe-Cr-C system.

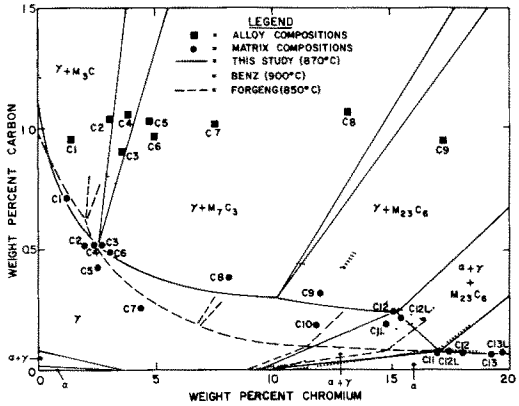

Fig. 5—The low-carbon, low-chromium region of the 870°C (1600°F) isothermal section of the Fe-Cr-C system.

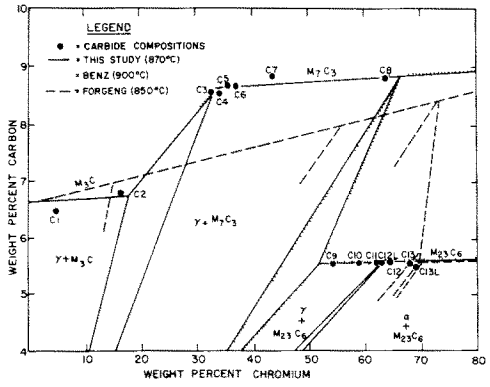

Fig. 6—The high-carbon region of the 870°C (1600°F) isothermal section of the Fe-Cr-C system.

ary compositions were determined by calculating the least-squares line through all microprobe analyses and known binary phase diagram data on the particular carbide. For example, the M_7C_3 phase boundary composition was determined by a least-squares line through the M_7C_3 compositions of alloys C3, C4, C5, C6, C7 and C8 and the Cr_7C_3 composition in the chromium-carbon system.

As shown in Fig. 7, the carbides were generally smaller than the 4 μm minimum required for quantitative microprobe analysis. However, in all alloys there were some carbides in the 4 to 10 μm size range. Alloys C3 and C4 had M_7C_3 and M_3C carbides coexisting, but all the large carbides were shown by selective etching to be M_7C_3. Therefore, no quantitative microprobe analysis of the M_3C carbides was possible in these two alloys. In all alloys, the quantity of extracted carbides was sufficient for the X-ray diffraction studies. Also, with the exception of alloy C1, the quantity of carbides extracted was also sufficient for wet chemical analysis.

The 870°C (1600°F) isotherm of the iron-chromium-carbon system determined in this study is quite similar to Benz's 900°C (1650°F) isotherm. It differs from Forgeng's 850°C (1560°F) isotherm in that the M_3C and M_7C_3 carbides are stoichiometric with regard to carbon rather than forming a pseudobinary system.

The compositions of the phase fields along the edges of the ternary phase diagram are known from the diagrams of the component binary systems.[13] Therefore, Point *A*, in the schematic diagram of Fig. 8, the Fe_3C

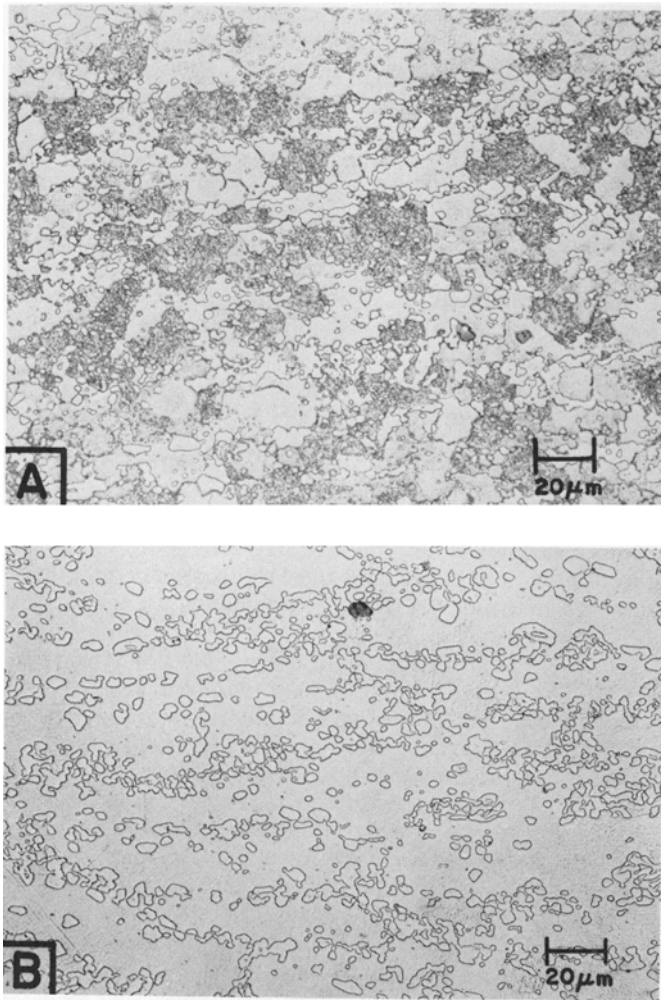

Fig. 7—Microstructures of the Fe-Cr-C alloys held 1000 h at 870°C (1600°F), picral/HCl etch, magnification 300 times. (*a*) Alloy C12 (0.94 pct C, 23.92 pct Cr) tempered 1 h at 200°C (400°F), (*b*) Alloy C13 (1.00 pct C, 28.87 pct Cr).

Table III. X-Ray Diffraction Analyses of Extracted Carbides

Alloy	Carbides Present	Relative Percentages	Lattice Parameter (A) a_0	b_0	c_0
C1	M_3C	100	4 53	5.09	6.73
C2	M_3C	100	4.51	5.07	6.70
C3	M_3C	6	4.52	5.08	6.69
	M_7C_3	94	13 91	–	4.55
C4	M_3C	75	4.51	5.07	6.69
	M_7C_3	25	13 93	–	4 55
C5	M_7C_3	100	13.94	–	4 56
C6	M_7C_3	100	13 95	–	4.60
C7	M_7C_3	100	13 99	–	4 54
C8	M_7C_3	100	14 27	–	4 71
C9	$M_{23}C_6$	100	10 60	–	–
C10	$M_{23}C_6$	100	10 60	–	–
C11	$M_{23}C_6$	100	10 61	–	–
C12	$M_{23}C_6$	100	10.61	–	–
C13	$M_{23}C_6$	100	10.63	–	–

Table IV. Carbide Contents of the Alloys

Alloy	Carbide Type	Extraction Wt Pct	Metallographic Vol Pct	Predicted by Proposed Diagram Wt Pct	Vol Pct
C1	M_3C	3.2	4 2	2 1	2 1
C2	M_3C	10.0	9 8	7.3	7 6
C3	Total	6 1	6 5	4.9	5 6
	M_3C	–	0.2	0.9	1 0
	M_7C_3	–	6.3	4 0	4 6
C4	Total	9 2	9 5	8 3	8.8
	M_3C	–	6 9	6.8	7 1
	M_7C_3	–	2.6	1 5	1.7
C5	M_7C_3	8 0	8.4	6.4	7 3
C6	M_7C_3	7 0	8.4	5.8	6.7
C7	M_7C_3	8 0	10 0	7 0	8.0
C8	M_7C_3	9 0	9 7	8 7	9.9
C9	$M_{23}C_6$	15.0	14.1	12 9	14.5
C10	$M_{23}C_6$	16 0	18 8	17.5	19.5
C11	$M_{23}C_6$	14 1	17.1	13 9	15.6
C12	$M_{23}C_6$	15.9	16.8	15.3	17.0
C13	$M_{23}C_6$	15 8	18.3	16 9	18 7

Table V. Compositions of Extracted Carbides

Alloy	Cr/(Cr + Fe)
C1	–
C2	0.160
C3	0.327
C4	0.231
C5	0 344
C6	0 327
C7	0 446
C8	0 627
C9	0 523
C10	0.579
C11	0 620
C12	–
C13	0 680

Table VI. Results of Microprobe Analyses

Alloy	Phase	Composition, Wt Pct C	Cr	Fe
C1	Austenite	0 71 ± 0 05	1 21 ± 0.04	95 53 ± 0.76
	M_3C	6.46 ± 0.05	7.53 ± 0.26	81.15 ± 3.68
C2	Austenite	0.53 ± 0.02	2.02 ± 0.02	97.42 ± 0.97
	M_3C	6 88 ± 0.05	16.71 ± 0.38	76 34 ± 0.90
C3	Austenite	0.53 ± 0.04	2.61 ± 0.06	95 01 ± 0.89
	M_7C_3	8.54 ± 0.07	32.41 ± 2.74	58.94 ± 5.17
C4	Austenite	0.52 ± 0.06	2.40 ± 0.26	94.34 ± 0.60
	M_7C_3	8.43 ± 0.13	33.02 ± 0 93	56.10 ± 0.66
C5	Austenite	0 43 ± 0.02	2.50 ± 0.09	96 34 ± 0.35
	M_7C_3	8 59 ± 0.36	34.33 ± 2.40	58 33 ± 0 42
C6	Austenite	0.49 ± 0 05	2.82 ± 0.09	92.74 ± 0.74
	M_7C_3	8.82 ± 0.13	35.78 ± 1.00	55.87 ± 0.70
C7	Austenite	0.25 ± 0.03	4.33 ± 0.32	85.67 ± 0 72
	M_7C_3	8.82 ± 0.07	43.16 ± 0.58	45.86 ± 3.56
C8	Austenite	0.39 ± 0.10	8.17 ± 0.41	88 98 ± 1.67
	M_7C_3	8.78 ± 0 12	63.89 ± 1.92	28.40 ± 0.77
C9	Austenite	0.33 ± 0.03	12.02 ± 0.19	82 02 ± 2.08
	$M_{23}C_6$	5.60 ± 0.20	54.14 ± 1.87	36 98 ± 0 79
C10	Austenite	0.18 ± 0.11	11.70 ± 0 72	83.67 ± 4.82
	$M_{23}C_6$	5.56 ± 0.07	58.39 ± 0.25	36 95 ± 0 41
C11	Austenite	0.18 ± 0.02	14.77 ± 1 14	79.43 ± 0.57
	Ferrite	0.05 ± 0.02	17.79 ± 0 71	82.39 ± 2.94
	$M_{23}C_6$	5.54 ± 0.11	61.22 ± 1.52	30 89 ± 2 17
C12	Austenite	0 26 ± 0 02	14.49 ± 0.21	86.22 ± 1.08
	Ferrite	0.09 ± 0 01	18.16 ± 0.50	83.49 ± 0.54
	$M_{23}C_6$	5 53 ± 0.16	63.87 ± 0.42	29 34 ± 0.73
C12L*	Austenite	0.21 ± 0 02	15 39 ± 0.33	85.12 ± 3.48
	Ferrite	0.07 ± 0.02	17.41 ± 0.60	80 23 ± 2.25
	$M_{23}C_6$	5.49 ± 0 09	62.10 ± 2 00	31 21 ± 5 53
C13	Ferrite	0.06 ± 0.01	19.30 ± 0 14	77.66 ± 0 74
	$M_{23}C_6$	5.58 ± 0.09	67 08 ± 0.45	26 33 ± 2 12
C13L*	Ferrite	0 07 ± 0 01	19.74 ± 0.16	78 52 ± 0.66
	$M_{23}C_6$	5.45 ± 0 09	68.58 ± 2.51	26.51 ± 1 79

*These data were determined with Lehigh's microprobe All other data were determined with Bethlehem Steel's microprobe.

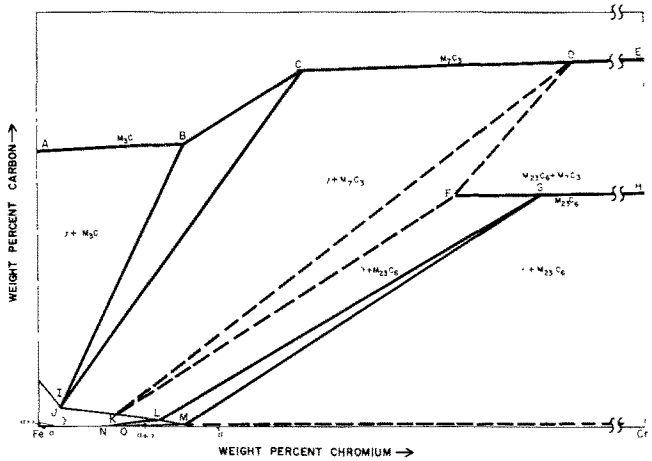

Fig. 8—Schematic drawing of the 870°C (1600°F) isothermal section of the Fe-Cr-C system.

composition in the Fe-C system, was plotted at 6.67 pct C. Similarly, Points *E* and *H* representing Cr_7C_3 and $Cr_{23}C_6$ in the Cr-C system was plotted at 9.0 and 5.68 pct respectively. Point *I*, representing the carbon solubility limit in γ iron, was plotted at 1.13 pct C. Finally, Point *N* for the $\gamma : \gamma + \alpha$ phase boundary and Point *O* for the $\gamma + \alpha : \alpha$ phase boundary in the Fe-Cr system were plotted at 9.0 and 10.0 pct Cr respectively.

The limit of iron substitution in the M_7C_3 carbide (Point *C*), which is also the M_7C_3 corner of the $\gamma + M_7C_3 + M_3C$ tie triangle, was determined by microprobe analysis of the M_7C_3 carbides in alloys C3 and C4. These alloys have compositions that fall within the $\gamma + M_7C_3 + M_3C$ tie triangle. As shown in Table VI, the M_7C_3 compositions in the two alloys were almost identical—32.41 pct Cr and 8.54 pct C as compared with 33.02 pct Cr and 8.43 pct. Furthermore, the average chromium content, 32.7 pct is in close agreement with the 33 pct reported by Benz.[8] The best estimate of the M_7C_3 compositions was obtained by calculating the composition at the intersection of the lines describing: 1) the M_7C_3 composition, and 2) the $\gamma - M_7C_3$ side of the $\gamma + M_3C + M_7C_3$ tie triangle. The resulting composition, 8.61 pct C and 33.20 pct Cr, was plotted on the diagram as Point *C*. This composition is equivalent to 29.92 at. pct carbon, which is quite close to the 30.0 at. pct required for carbide stoichiometry and confirms Benz's suggestion that the carbides are stoichiometric with respect to carbon.

Point *B*, the limit of chromium substitution in the M_3C phase is another corner of the $\gamma + M_3C + M_7C_3$ tie triangle and could not be determined by microprobe analysis. The M_3C carbides were too small for quantitative microprobe analysis. However, the composition of the M_3C carbides was obtained from a materials balance, and the $Cr/(Cr + Fe)$ ratio for the M_3C carbides in alloy C4 was calculated to be 0.184. Assuming carbon stoichiometry, this ratio is equivalent to 17.15 pct Cr. Since this is close to the 18 pct of Jackson and Benz, Point *B* was plotted at 18 pct Cr to be consistent with the published diagrams and at 6.81 pct C, which is the value for 18 pct Cr on the least-squares line describing the M_3C compositions. This composition is equivalent to 25.11 at. pct C, which is almost exactly the 25.0 pct required for a stoichiometric M_3C carbide. Thus, the M_3C composition also indicates that the M_3C and M_7C_3 carbides do not form a pseudobinary system.

Point *D*, the M_7C_3 corner of the $\gamma + M_7C_3 + M_{23}C_6$ tie triangle, could not be determined from our data because none of the alloys had compositions that fell within that tie triangle. However, we know that the chromium content at that point must be above 63.9 pct, because that concentration was observed in the M_7C_3 carbides of alloy C8, which lies in the $\gamma + M_7C_3$ phase field. Point *D* was therefore plotted at 65.7 pct Cr to be consistent with the diagram of Benz *et al* and at 8.84 pct C, which is the 65.7 pct Cr point on the least-squares line describing the M_7C_3 compositions.

For the same reasons, Point *F*, is the maximum iron content permitted in the $M_{23}C_6$ carbide and is another corner of the same tie triangle that contains Point *D*. Point *F* also could not be determined from our data. From microprobe analyses of $M_{23}C_6$ car-

bides in alloy C9, which is the nearest alloy in the $\gamma + M_{23}C_6$ phase field, we know that the chromium content of Point F must be less than 54.1 pct. In the absence of other evidence, Point F was plotted at 51.7 pct Cr and 5.51 pct C to have a chromium content consistent with that estimated by Benz and at the carbon content described by the least-squares line through the $M_{23}C_6$ compositions. This composition, which is equivalent to 20.69 at. pct C and is stoichiometric with respect to carbon, differs greatly from the 70 pct Cr proposed by Forgeng.[5]

The $M_{23}C_6$ corner of the $\alpha + \gamma + M_{23}C_6$ tie triangle (Point G) was set at a composition of 62.78 pct Cr and 5.55 pct C by averaging the compositions at the intersections of the least-squares lines that describe 1) the $M_{23}C_6$ composition, 2) the $\gamma - M_{23}C_6$ side of the tie triangle, and 3) the $\alpha - M_{23}C_6$ side of the tie triangle. This composition is very close to the 62.0 pct Cr estimated from Benz's data but, again, is significantly lower than the 70 pct Cr shown by Forgeng.

The composition of Point J, the austenite corner of the $\gamma + M_3C + M_7C_3$ tie triangle, was determined to be 2.50 pct Cr and 0.53 pct C by averaging the microprobe analyses of the austenite of alloys C3 and C4. These alloys were shown by X-ray diffraction study of extracted carbides to lie within the $\gamma + M_3C + M_7C_3$ tie triangle. Given the temperature differences, this composition is in good agreement with those shown by Forgeng and Benz.

Point K, the austenite corner of the $\gamma + M_7C_3 + M_{23}C_6$ field, could not be determined from our alloys, because none had compositions within that three-phase field. As shown in Fig. 4, Point K was assigned a composition of 10.0 pct Cr and 0.3 pct C to be consistent: a) with the composition of the austenite in alloy C8 where the austenite coexisted with M_7C_3 carbides and with that of alloy C9 which contained $M_{23}C_6$ carbides, and b) with the published diagram sections at temperatures bracketing our 870°C section.

The compositions of Points L and M, which are the austenite and ferrite corners of the $\alpha + \gamma + M_{23}C_6$ tie triangle, were determined to be 14.78 pct Cr, 0.22 pct C and 17.75 pct Cr, 0.07 pct C respectively. The austenite composition was determined by averaging the austenite compositions of alloys C11 and C12. The ferrite composition was determined by calculating the composition at the intersection of the least-squares lines describing a) the ferrite composition and b) the ferrite-$M_{23}C_6$ side of the tie triangle.

SUMMARY AND CONCLUSIONS

The 870°C (1600°F) isothermal section of the ternary iron-chromium-carbon system was developed with metallographic, carbide extraction, X-ray and quantitative electron microprobe techniques. Tie lines are presented for 9 two-phase alloys in the system. Also, the compositions at the corners of the $\alpha - \gamma - M_{23}C_6$ and $\gamma - M_3C - M_7C_3$ tie triangles were determined. Significant new information about this system includes:

1) The M_3C and M_7C_3 carbides are stoichiometric with respect to carbon. Most published diagrams for isothermal sections at comparable temperatures show these carbides forming a pseudobinary system.

2) The solubility limits for iron in the carbides are:

Carbide	Iron Solubility Limits, Pct
M_3C	75.2 to 93.3
M_7C_3	0.0 to 58.2
$M_{23}C_6$	0.0 to 42.8

In addition, this work confirms the findings of previous investigators that: 1) the only carbides present in the system are M_3C, M_7C_3 and $M_{23}C_6$, and 2) $M_{23}C_6$ carbides are in equilibrium with both α and γ whereas M_3C and M_7C_3 are in equilibrium with γ only.

ACKNOWLEDGMENTS

The authors are grateful to the Bethlehem Steel Corporation for the use of the facilities of the Homer Research Laboratories and the sponsorship of Woodyatt's PhD program at Lehigh University and to Lehigh University for the use of their facilities. Acknowledgments are also due to many of Woodyatt's coworkers, including W. C. Bleam, A. B. Gackenbach, J. T. Gallagher, J. R. Kilpatrick, M. H. Longenbach and L. R. Salvage for their assistance in gathering the data. Particular thanks must go to T. R. Knauss for his valuable assistance throughout this effort.

REFERENCES

1. W Tofaute, A Sponheuer, and H. Bennek. *Arch. Eisenhuttenw.*, 1935, vol 8, pp. 499-506.
2. W. Tofaute, G. Kuttner, and A. Buttinghaus *Arch. Eisenhuttenw.*, 1936, vol. 9, pp. 607-16.
3. K. Bungardt, E Kunze, and E. Horn *Arch. Eisenhuttenw*, 1958, vol. 29, pp 193-203.
4. R. S. Jackson *J. Iron Steel Inst*, 1970, vol. 208, pp. 163-67.
5. W D. Forgeng and W. D. Forgeng, Jr *Metals Handbook*, vol. 8, pp. 402-04, ASM, Metals Park, Ohio
6. R. Benz, J F Elliott, and J. Chipman *Met Trans*, 1974, vol. 5, pp. 2235-40.
7. O H. Kriege *Metallography—A Practical Tool for Correlating the Structure and Properties of Materials*, STP 557, pp 220-32, American Society for Testing and Materials, Philadelphia, Penn, 1973.
8. _____, ASTM Powder Diffraction File, Joint Committee on Powder Diffraction Standards, Swathmore, Penn., 1973.
9. C S Barrett. *Structure of Metals*, pp. 149-50, McGraw-Hill Book Co., New York, N.Y, 1952.
10. J I. Goldstein and P. A. Comella *A Computer Program for Electron Probe Microanalysis in the Fields of Metallurgy and Geology*, Report X-642-69, 115, Goddard Space Flight Center, 1969
11. B. L. Henke and E. S Ebisu. *Advances in X-Ray Analysis*, vol. 17, pp. 150-213, Plenum Press, New York, N Y., 1974.
12. R. W. Gurry, J Christakos, and L. S Darken *Trans ASM*, 1961, vol. 53, pp 187-98
13. D B. Clayton, T. B. Smith, and J. R Brown: *J. Inst Metals*, 1961-62, vol. 90, pp 224-33.